4096-ary OCDM at 2.5 Gbit/s using multidimensional PSK codes with a single multi-port encoder/decoder

Takahiro Kodama[1], Nobuyuki Kataoka[2], Naoya Wada[2], Gabriella Cincotti[3], Xu Wang[4], and Ken-ichi Kitayama[1]

1.Department of Electrical, Electronics and Information Engineering, Osaka University, Osaka 565-0871, Japan
2.National Institute of Information and Communications Technology (NICT), 4-2-1 Nukui-Kitamachi, Koganei, Tokyo 184-8795 Japan
3. Department of Applied Electronics, University Roma Tre, via della Vasca Navale 84, I-00146 Rome, Italy
4. School of Engineering and Physical Sciences, Heriot-Watt University, Riccarton, EH14 4AS, Edinburgh, U. K.
e-mail kodama@pn.comm.eng.osaka-u.ac.jp

Abstract: A record 4096 (=16X16X16)-ary OCDM system at 2.5Gbps using multidimensional phase shift keying (PSK) codes with a single multi-port optical encoder/decoder has been demonstrated for the first time. An accurate model evaluates the power margins.

OCIS codes: (060.2330) Fiber optics communications; (060.4230) Multiplexing; (060.4785) Optical security and encryption.

1. Introduction

Optical code division multiplexing (OCDM) is a flexible multiple access network that allows all the user to transmit on a single fiber and a single wavelength, by using optical codes (OC). One of its inherent advantages is the data confidentiality, because messages are encoded at the transmitter and can be recovered only by an authorized user, who knows the OC. On-off keying (OOK), differential-phase-shift-keying (DPSK) and code-shift-keying (CSK)-OCDM systems have been investigated and experimentally demonstrated during the past decade [1,2] and a careful security analysis has shown that the conventional OCDM bit-ciphering, where each bit is transformed into an OC, is not resistant against many confidentiality attacks [3-7]. Block-ciphering (or M-ary OCDM) is a more secure encoding method that transforms different sequences of $\log_2 M$ bits into different OCs. Fig. 1(a) shows the operation principle of M-ary OCDM [8-10]. This scheme presents two levels of confidentiality: physical-layer security, because an adversary should be able to correctly detect the OC, and computational security, since he or she does not know which sequence of bits corresponds to a given OC, and the number of possible combinations equates M!. Recently, 2.5Gbit/s, 16-ary OCDM transmission over a 50 km link has been experimentally demonstrated, using a single multi-port arrayed waveguide grating (AWG)- based encoder/decoder (E/D), that can simultaneously generates and decodes as many codes as the number of its ports [11]. Since the number of OCs is limited by the port count, it would be desirable if the M-ary number could be increased without increasing the number of OCs.

To make M-ary OCDM scalable in M count multidimensional PSK codes M-ary OCDM that is shown Fig. 1(b) had proposed [12, 13], but, to the best of our knowledge, it has been not experimentally demonstrated yet. In the present paper, we demonstrate for the first time the operation principle of 4096 (= 16X16X16)-ary OCDM at 2.5 Gbps using multidimensional PSK codes generated by a multi-port optical E/D. Note that the number of OCs required, 4096, surpasses far beyond a conventional optical E/D device technology, which generate a few hundreds codes at most. Finally, the influence of multiple interference is theoretically and analytically analyzed.

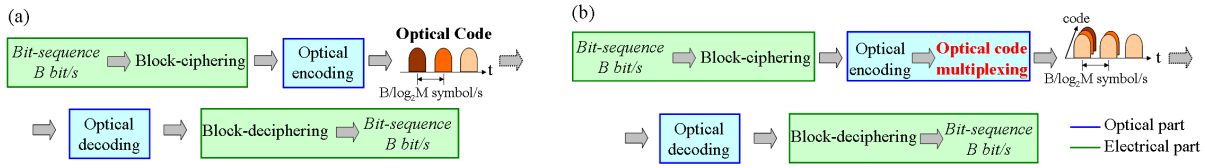

Fig. 1. (a) Scheme of conventional M-ary OCDM. (b) Scheme of multidimensional PSK codes M-ary OCDM.

2. System configuration and operation principle

Figure 2 shows the architecture and the operation principle of a multidimensional PSK 4096-ary OCDM system. At the transmitter, a serial data bit stream at B bit/s is segmented every 12 bits by a serial-to-parallel (SP) converter and each 12-bit block is sent to a 12-to-15 line coder. The former 4-bit block (high-order bits: HX), the medium 4-bit block (middle-order bits: MX) and the latter 4-bit block (lower-order bits: LX) are mapped onto three codewords, according to the code lookup table (as shown in inset table of Fig. 2). We observe that the code lookup table can be suitably selected and a message of 12 bits can be decomposed in three parts of 4 bits each in a complete arbitrary way.

JWA38.pdf

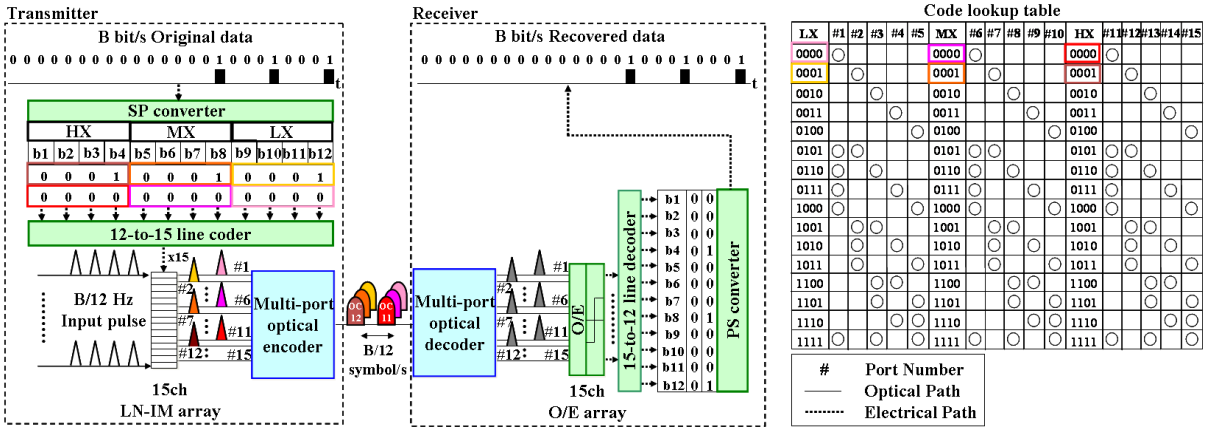

Fig. 2. Architecture of 4096-ary OCDM system.

Each output of line coder is connected to one of 15 ports of a $LiNbO_3$ intensity modulator (LN-IM) array, to generate a gate signal that selects an optical seed pulse corresponding to the OC. In the optical domain, the optical seed pulses at B/12 Hz are launched into 15ch LN-IM array, and only optical pulses passing through the optical gate are forwarded to a designated input port of the multi-port optical encoder. At the encoder output port, the codes corresponding to the optical seed pulses passed through the LN-IM are, and the selection of the input ports of the multi-port optical encoder determines which OCs are generated. The code repetition rate is equal to the symbol rate at B/12 Symbol/s.

At the receiver, the 4096-ary OCDM signal is processed by the multi-port optical decoder, which has the same configuration as the encoder. The auto-correlation waveforms appear at the decoder output ports corresponding to the transmitted OCs and the output port number unequivocally identifies the OC. The output optical pulse from the decoder is converted into an electrical signal by the 15-channel optical-to-electrical (O/E) converter array, and then launched into the 15-to-12 line decoder, so that the original 12 bit data sequence is recovered via the parallel-to-serial (PS) converter, using the same code lookup table.

3. Proof-of-concept demonstration

Figure 3 shows the experimental setup of the 4096-ary OCDM transmitter, where the fixed 96-bit data pattern, which includes all the codes in a period (shown in the inset (i)) has been used. At the transmitter, the serial data bit stream at 2.48832 Gbit/s is segmented every 12 bits by the SP converter; for convenience sake of the implementation of FPGA-based line coder the 12-bit sequence is then divided into 4-bit blocks, and each 4-bit block is separately mapped onto the combination of 15 OCs, according to the code lookup table by the FPGA-based line coder. Gate signals generated from the corresponding output of the line coder are used to drive the 15-channel LN-IM array. Inset (ii) of Fig. 3 shows the gate signals at each output of the 12-to-15 line coder. We used a super continuum (SC) light source, which consists of a mode-locked laser diode (MLLD), an erbium-doped fiber amplifier (EDFA), and a 2-km dispersion-flattened fiber (DFF). The MLLD at 1565 nm is driven at 9.95328 GHz. The SC

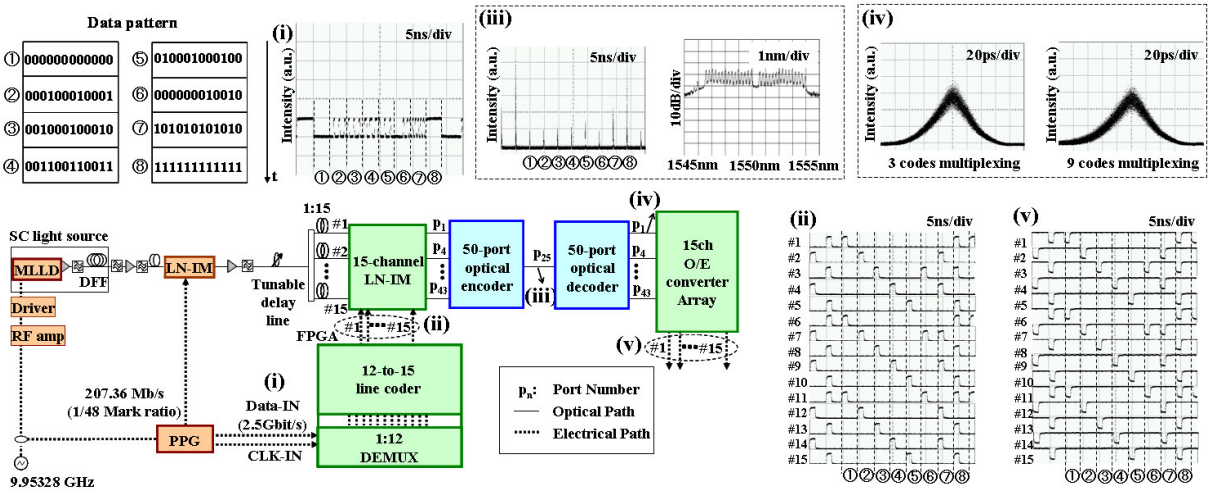

Fig. 3. Experimental setup of 4096-ary OCDM system.

signal is fed into an optical band-pass filter (OBPF) with 7.5 nm bandwidth at the center wavelength of 1550 nm. The pulse streams are down-converted to 207.36 MHz by a LN-IM, and split into 15 arms by optical couplers. Each arm is connected to a LN-IM: the pulse pattern passes through only if its arrival time corresponds to the gate signal pattern from the line coder. Each output of the LN-SWs is connected to a different input port of the multi-port encoder; we used 15 input ports (every 3 port) of a 50 X 50 multiport encoder/decoder. We obtain the multidimensional code signals Inset (iii) of Fig. 3 shows the waveform and spectrum of the generated 4096-ary OCDM signal. At the receiver, the 4096-ary OCDM signal is sent into the input of the multi-port optical decoder. The auto-correlation waveforms appear at the 15 output ports, and the output port number indicates the received OC. The left figure of inset (iv) shows the auto-correlation waveforms in the case of 3 OCs multiplexed. The right figure of inset (iv) shows the auto-correlation waveform in the case of 9 OCs. The output optical pulses from the multi-port optical decoder are converted into an electrical signal by the 15-channel O/E converter array (as shown in Fig. 3 (v)). All electrical gate signal patterns are clear opening and fully identified with that of the gate signals at the transmitter (Fig. 3 (ii)). This result proves the operation of this system is achieved successfully, although the BER measurements were not be able to conduct due to the failure of the clock recovery.

4. Analysis of cross-correlation and beat noise effect by optical code multiplexing

To numerically evaluate the performance of the M-ary transmission, we determine the signal Z from each output of 15ch O/E converter array as [14, 15]:

$$Z = \Re\int_0^{T_s}\left[\sum_{j=0}^{N-1}[(j+1)\exp(-\frac{(t-j\Delta\tau)^2}{2T_0^{\,2}})]^2 + \sum_{j=N}^{2N-2}[(2N-j-1)\exp(-\frac{(t-j\Delta\tau)^2}{2T_0^{\,2}})]^2\right]dt + \Re\int_0^{T_s}\sum_{n=1}^{m}\sum_{j=0}^{2N-2}[\frac{\sin\left[\frac{\pi(j+1)(k_n-k')}{N}\right]}{\sin\left[\frac{\pi(k_n-k')}{N}\right]}\exp(-\frac{(t-j\Delta\tau)^2}{2T_0^{\,2}})]^2 dt$$

Auto correlation 1 Auto correlation 2 Cross correlation

$$+2\Re\int_0^{T_s}\sum_{n=1}^{m}\sum_{j=0}^{N-1}(j+1)\frac{\sin\left[\frac{\pi(j+1)(k_n-k')}{N}\right]}{\sin\left[\frac{\pi(k_n-k')}{N}\right]}\cos\left[\frac{2\pi(j+1)}{N}(1+\frac{3(k'-k_n)}{2})-\frac{\pi(k_n-k')}{2N}\right]\exp(-\frac{2(t-j\Delta\tau)^2}{2T_0^{\,2}})dt$$

Auto correlation – cross correlation beat term 1

$$+2\Re\int_0^{T_s}\sum_{n=1}^{m}\sum_{j=N}^{2N-2}(2N-j-1)\frac{\sin\left[\frac{\pi(j+1)(k_n-k')}{N}\right]}{\sin\left[\frac{\pi(k_n-k')}{N}\right]}\cos\left[\frac{2\pi(j+1)}{N}(1+\frac{3(k'-k_n)}{2})-\frac{\pi(k_n-k')}{2N}\right]\exp(-\frac{2(t-j\Delta\tau)^2}{2T_0^{\,2}})\,dt$$

Auto correlation – cross correlation beat term 2

$$+2\Re\int_0^{T_s}\sum_{n=1}^{m-1}\sum_{l=n+1}^{m}\sum_{j=0}^{2N-2}\frac{\sin\left[\frac{\pi(j+1)(k_n-k')}{N}\right]}{\sin\left[\frac{\pi(k_n-k')}{N}\right]}\frac{\sin\left[\frac{\pi(j+1)(k_l-k')}{N}\right]}{\sin\left[\frac{\pi(k_l-k')}{N}\right]}\cos[\frac{\pi(2j+3)}{N}(k_l-k_n)]\exp(-\frac{2(t-j\Delta\tau)^2}{2T_0^{\,2}})\,dt$$

Cross correlation – cross correlation beat term

where N is the total port number, $\Delta\tau$ is the time distance between two chip pulses in each code, $\Re$ is the responsibility of the photodetector, T_s is the symbol duration, T_0 is the pulse width, j is the chip pulse number and k, k' are respectively the input number of encoder and the output number of decoder. Figure 4 shows the power margin between the 0 level signal (related to only cross correlations) and the 1 level signal (related to the auto correlation). The values of power margin are larger than 9.2 dB for all ports. This result shows that 0 level and 1 level signals can be easily determined, by properly setting the threshold.

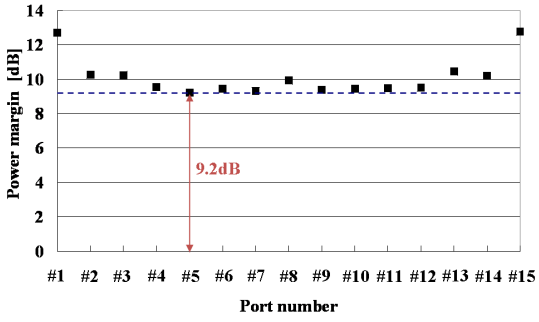

Fig. 4. Power margin at each port.

5. Conclusions

We have successfully demonstrated the proof-of-concept of a multidimensional PSK codes 4096-ary, 207.36MSymbol/s, coherent OCDM-based block ciphering. In addition, simulation results showed power margins between 0 level and 1 level in each port are very high.

6. References

1 G. Manzacca *et al.*, *PTL.*, vol. 19, no. 8, pp. 559-561, 2007.
2 X. Wang *et al.*, *ECOC2006*, 2006.
3 T. H. Shake, *JLT.*, vol. 23, no. 2, pp. 655-670, 2005.
4 T. H. Shake, *JLT.*, vol. 23, no. 4, pp. 1652-1663, 2005.
5 D. E. Leaird *et al.*, *EL.*, vol. 41, no. 14, pp. 817-819, 2005.
6 X. Wang *et al.*, *J. STQE.*, vol. 13, no. 5, pp. 1463-1470, 2007.
7 G. Cincotti *et al.*, *JLT.*, vol. 26, no. 13, pp. 1798-1806, 2008.
8 E. Narimanov *et al.*, *2005 QELS.*, JThE70, 2005.
9 S. Galli *et al.*, *IEEE Globecom.*, vol. 4, pp. 2009-2013, 2005.
10 R. Menendez *et al.*, *J. ON*, vol. 6, Issue 5, pp. 442-450, 2007.
11 T. Kodama *et al.*, *JLT.,* vol. 28, no. 1, pp. 181-187, 2010.
12 N. Kataoka *et al.*, *ECOC 2007* Tu3.2.6, 2007.
13 G. Cincotti *et al.*, *JLT.,* vol. 26, no. 13, pp. 1798-1806, 2008.
14 G. Cincotti *et al.*, *JLT.,* vol. 24, no. 1, pp. 103-112, 2006.
15 X. Wang *et al.*, *JLT.,* vol. 22, no. 10, pp. 2226-2235, 2004.